JACC: ADVANCES VOL. 3, NO. 10, 2024

ORIGINAL RESEARCH

DPD Quantification Correlates With Extracellular Volume and Disease Severity in Wild-Type Transthyretin Cardiac Amyloidosis

René Rettl, MD, PhD,[a] Raffaella Calabretta, MD, PhD,[b] Franz Duca, MD, PhD,[a] Christina Kronberger, MD,[a] Christina Binder, MD, PhD,[a] Robin Willixhofer, MD,[a] Michael Poledniczek,[a] Felix Hofer, MD, PhD,[a] Carolina Doná, MD,[a] Dietrich Beitzke, MD,[c] Christian Loewe, MD,[c] Christian Nitsche, MD, PhD,[a] Christian Hengstenberg, MD,[a] Roza Badr Eslam, MD,[a] Johannes Kastner, MD,[a] Jutta Bergler-Klein, MD,[a] Marcus Hacker, MD,[b] Andreas A. Kammerlander, MD, PhD[a]

ABSTRACT

BACKGROUND The pathophysiological hallmark of wild-type transthyretin amyloid cardiomyopathy (ATTRwt-CM) is the deposition of amyloid within the myocardium.

OBJECTIVES This study aimed to investigate associations between quantitative cardiac ^{99m}Tc-3,3-diphosphono-1,2-propanodicarboxylic acid (DPD) uptake and myocardial amyloid burden, cardiac function, cardiac biomarkers, and clinical status in ATTRwt-CM.

METHODS Forty ATTRwt-CM patients underwent quantitative DPD single photon emission computed tomography/computed tomography to determine the standardized uptake value (SUV) retention index, cardiac magnetic resonance imaging to determine extracellular volume (ECV) and cardiac function (RV-LS), and assessment of cardiac biomarkers (N-terminal prohormone of brain natriuretic peptide [NT-proBNP], troponin T) and clinical status (6-minute walk distance [6MWD], National Amyloidosis Centre [NAC] stage). ATTRwt-CM patients were divided into 2 cohorts based on median SUV retention index (low uptake: $<$5.19 mg/dL, n = 20; high uptake: $\geq$5.19 mg/dL, n = 20). Linear regression models were used to assess associations of the SUV retention index with variables of interest and the Mann-Whitney U or chi-squared test to compare variables between groups.

RESULTS ATTRwt-CM patients (n = 40) were elderly (78.0 years) and predominantly male (75.0%). Univariable linear regression analyses revealed associations of the SUV retention index with ECV (r = 0.669, β = 0.139, $P < 0.001$), native T1 time (r = 0.432, β = 0.020, $P = 0.005$), RV-LS (r = 0.445, β = 0.204, $P = 0.004$), NT-proBNP ($\log_{10}$) (r = 0.458, β = 2.842, $P = 0.003$), troponin T (r = 0.422, β = 0.048, $P = 0.007$), 6MWD (r = 0.385, β = −0.007, $P = 0.017$), and NAC stage (r = 0.490, β = 1.785, $P = 0.001$). Cohort comparison demonstrated differences in ECV ($P = 0.001$), native T1 time ($P = 0.013$), RV-LS ($P = 0.003$), NT-proBNP ($P < 0.001$), troponin T ($P = 0.046$), 6MWD ($P = 0.002$), and NAC stage (I: $P < 0.001$, II: $P = 0.030$, III: $P = 0.021$).

CONCLUSIONS In ATTRwt-CM, quantitative cardiac DPD uptake correlates with myocardial amyloid load, longitudinal cardiac function, cardiac biomarkers, exercise capacity, and disease stage, providing a valuable tool to quantify and monitor cardiac disease burden. (JACC Adv. 2024;3:101261) © 2024 The Authors. Published by Elsevier on behalf of the American College of Cardiology Foundation. This is an open access article under the CC BY-NC-ND license (http://creativecommons.org/licenses/by-nc-nd/4.0/).

ISSN 2772-963X https://doi.org/10.1016/j.jacadv.2024.101261

ABBREVIATIONS AND ACRONYMS

ATTRwt-CM = wild-type transthyretin amyloid cardiomyopathy

CA = cardiac amyloidosis

CMR = cardiac magnetic resonance

DPD = ^{99m}Tc-3,3-diphosphono-1,2-propanodicarboxylic acid

ECV = extracellular volume

NAC = National Amyloidosis Centre

PYP = ^{99m}Tc-pyrophosphate

SPECT/CT = single photon emission computed tomography/computed tomography

SUV = standardized uptake value

VOI = volume of interest

The pathophysiological hallmark of transthyretin amyloid cardiomyopathy (ATTR-CM) is characterized by the accumulation of misfolded transthyretin (TTR) deposited extracellularly as amyloid fibrils in the myocardium, leading to progressive heart failure with fatal prognosis.[1,2] Despite diagnostic challenges, nuclear imaging utilizing semiquantitative bone scintigraphy with amyloid-avid tracers such as ^{99m}Tc-3,3-diphosphono-1,2-propanodicarboxylic acid (DPD) has emerged as the noninvasive gold standard for the diagnosis of ATTR-CM in recent years.[3,4] Advanced quantitative single-photon emission computed tomography/computed tomography (SPECT/CT) with DPD overcomes several limitations of semiquantitative bone scintigraphy by providing 3-dimensional visualization of tracer uptake in the body and is recommended to aid in the diagnosis and quantification of cardiac disease burden in ATTR-CM.[5-8] In particular, the determination of a standardized uptake value (SUV), which indicates the concentration of the radiopharmaceutical in each tissue, may be useful in quantifying myocardial amyloid burden.[6-8] Cardiac magnetic resonance (CMR) imaging with T1 mapping has already been validated as an accurate, noninvasive approach to quantify myocardial amyloid load in patients with cardiac amyloidosis (CA) by determining myocardial extracellular volume (ECV),[9,10] which has been shown to correlate with histological ECV obtained from CA endomyocardial specimens.[11,12] However, data regarding the association of quantitative cardiac tracer uptake with amyloid burden in the myocardium remain limited.[13,14]

Therefore, the present study aimed to investigate the relationship between quantitative cardiac DPD uptake and myocardial amyloid load, as assessed by CMR-derived ECV, as well as cardiac function, cardiac biomarkers, and clinical status in patients with wild-type ATTR-CM (ATTRwt-CM) and to identify nuclear imaging biomarkers for quantifying cardiac disease burden.

METHODS

STUDY DESIGN. The present imaging study was conducted within the framework of a prospective heart failure registry at the Department of Internal Medicine II, Division of Cardiology, Medical University of Vienna, Austria, which includes a dedicated amyloidosis outpatient clinic. The local ethics committee (#796/2010) granted approval for this study, aligning with the principles of the Declaration of Helsinki. All participants provided written informed consent prior to enrollment.

STUDY POPULATION. Consecutive registry patients with a diagnosis of ATTR-CM between February 2019 and April 2021 were assessed for study eligibility. ATTR-CM patients were excluded if the following criteria were fulfilled: 1) inability to undergo DPD SPECT/CT imaging; 2) inability to undergo CMR imaging; 3) possession of a mutation in the TTR gene (ATTRv-CM); this subset of patients is notably diverse, with an individual, mutation-dependent, and markedly variable disease course compared to ATTRwt-CM; and 4) treatment with disease-specific therapies prior to baseline assessment. Eligible study participants underwent baseline examinations, including DPD SPECT/CT and CMR imaging, along with clinical and laboratory assessments at our dedicated amyloidosis outpatient clinic as part of a prospective investigational imaging study.

DIAGNOSIS OF TRANSTHYRETIN AMYLOID CARDIOMYOPATHY. Bone scintigraphy was performed in patients with clinical evidence of CA according to the noninvasive diagnostic algorithm proposed by Gillmore et al.[4] ATTR-CM was diagnosed when patients had significant cardiac tracer uptake (Perugini grade ≥2) on bone scintigraphy,[3] alongside the absence of paraprotein or monoclonal protein detected by serum and urine immunofixation and serum free light chain assay.[4] All patients diagnosed with ATTR-CM were offered the option of TTR gene sequencing, which was accepted by all individuals. Of the 71 ATTR-CM patients screened for study eligibility, 4 (5.6%) ATTR-CM patients had a mutation in the TTR gene (ATTRv-CM).

From the [a]Division of Cardiology, Department of Internal Medicine II, Medical University of Vienna, Vienna, Austria; [b]Division of Nuclear Medicine, Department of Biomedical Imaging and Image-guided Therapy, Medical University of Vienna, Vienna, Austria; and the [c]Division of Cardiovascular and Interventional Radiology, Department of Biomedical Imaging and Image-guided Therapy, Medical University of Vienna, Vienna, Austria.

The authors attest they are in compliance with human studies committees and animal welfare regulations of the authors' institutions and Food and Drug Administration guidelines, including patient consent where appropriate. For more information, visit the Author Center.

Manuscript received March 20, 2024; revised manuscript received August 1, 2024, accepted August 12, 2024.

DPD SCINTIGRAPHY AND SPECT/CT IMAGING. Nuclear imaging was performed at the Division of Nuclear Medicine, Department of Biomedical Imaging and Image-guided Therapy, Medical University of Vienna. A hybrid SPECT/CT system (Symbia Intevo, Siemens Medical Solutions AG) equipped with a low-energy, high-resolution collimator (dose length product [DLP]: 84.0 mGy/cm, IQR: 63.3-99.0) was used to obtain planar whole-body scintigraphy images 2.5 hours and SPECT/CT images of the thorax 3.0 hours after intravenous injection of DPD (DPD activity: 725.0 MBq, IQR: 708.0-738.5). Images were captured in a 180° configuration, comprising 64 views with a duration of 20 seconds per view, a 256×256 matrix, and an energy window of 15% around the DPD photopeak of 141 keV. After the SPECT acquisition, a low-dose CT scan was obtained for attenuation correction, using settings of 130 kV, 35 mAs, a 256×256 matrix, and a step-and-shoot acquisition with body contour. Image acquisition and reconstruction were performed using xSPECT/CT QUANT (xQUANT) technology (eight iterations, 4 subsets, 3.0 mm smoothing filter, and a 20 mm Gaussian filter), which uses a 3% National Institute of Standards and Technology traceable precision source to standardize uptake values across different cameras, dose calibrators, and equipment.[15,16]

QUANTIFICATION OF CARDIAC DPD UPTAKE. Dedicated software (Hermes Hybrid 3D software, Hermes Medical Solutions) was used to quantify tracer uptake on SPECT/CT images. Three-dimensional volumes of interest (VOI) of left ventricular (LV) myocardium were automatically generated by dedicated software using a threshold-based method (39% of maximal activity) as previously described,[6-8] allowing clear separation of LV wall from LV cavity blood pool activity, as shown in Supplemental Figure 1. The VOIs of the LV myocardium were reviewed by the operator and corrected if there was evident sternal or rib uptake. From these VOIs, a SUV was calculated, which indicates the concentration of the radiopharmaceutical in the respective tissue, with the SUV peak representing the highest average SUV within a 1 cm^3 volume.[6-8] Bone uptake (SUV peak vertebral) was calculated by placement of a cubic 2.92 mL VOI in an intact vertebral body of a thoracic spine in an area without degenerative changes to minimize bias from high degenerative tracer accumulation.[6-8] To determine the SUV peak of the paraspinal muscle, a cubic 1.19 mL VOI was placed in the left paraspinal muscle.[6-8] Confounding from competing tracer uptake between tissues can be overcomed by a composite SUV retention index that balances uptake between the heart, bone, and soft tissue compartments.[6-8] It has been calculated using the following formula:

$$\text{SUV retention index} = \left(\frac{\text{SUV peak cardiac}}{\text{SUV peak vertebral}}\right) \times \text{SUV peak paraspinal muscle}$$

Planar whole-body scintigraphy images were independently assessed by 2 experienced nuclear medicine physicians and visually graded according to Perugini et al;[3] discrepancies were resolved by consensus. SPECT/CT images of the thorax were analyzed with dedicated software (Hermes Hybrid 3D software, Hermes Medical Solutions) and evaluated by 2 independent experienced observers.

CARDIAC MAGNETIC RESONANCE IMAGING. CMR imaging was performed in ATTRwt-CM patients without contraindications, such as chronic kidney disease stage 4 or 5 with an estimated glomerular filtration rate <30 mL/min/1.73 m^2 or those with implanted cardiac devices, using a 1.5-T scanner (MAGNETOM Avanto Fit, Siemens GmbH) according to standard protocols,[17] including late gadolinium enhancement and T1 mapping to determine T1 times. For cine imaging, steady-state free precision images were used (repetition time msec/echo time msec, 3.2/1.2; flip angle, 64°; voxel size, 1.4 × 1.4 × 6 mm; matrix, 180 × 256 pixels). For late gadolinium enhancement imaging, segmented inversion recovery sequences (700/1.22; flip angle, 50°; voxel size, 1.4 × 1.4 × 8 mm; 146 × 256 matrix) were performed at least 10 minutes after injection of 0.1 mmol/mL gadobutrol (Gadovist, Bayer Vital GmbH). T1 mapping was performed with electrocardiographically triggered modified look-locker inversion recovery sequence with a 5(3)3 prototype (5 acquisition heartbeats followed by 3 recovery heartbeats and a further 3 acquisition heartbeats) on a short-axis mid-cavity slice and with a 4-chamber view. T1 maps were created both before and 15 minutes after contrast agent application. For postcontrast T1 mapping, a 4(1)3(1)2 prototype was used. To counteract the patchy distribution of amyloid within the myocardium, regions of interest in our T1 maps included the whole myocardium (excluding the endocardium) in mid-cavity short-axis views and 4-chamber views. T1 values from the short-axis and the 4-chamber view were averaged. ECV was calculated using the following formula:[18]

$$\text{ECV} = (1 - \text{hematocrit}) \times \frac{\left(\frac{1}{T1\ \text{myo post}}\right) - \left(\frac{1}{T1\ \text{myo pre}}\right)}{\left(\frac{1}{T1\ \text{blood post}}\right) - \left(\frac{1}{T1\ \text{blood pre}}\right)}$$

For conventional hematocrit measurement, venous blood was collected from all patients during

intravenous line placement for contrast administration. LV mass was calculated from total myocardial volume multiplied by the specific gravity of the myocardium (1.05 g/mL) and indexed to body surface area (LV mass index). LV and right ventricular (RV) endocardial and epicardial contours were manually traced on the short-axis slice stacks during end-systole and end-diastole using dedicated software to quantify LV and RV function and volumes. LV global longitudinal strain (GLS) was calculated using 3 long-axis views (2-chamber, 3-chamber, and 4-chamber). GLS values were averaged from peak values of all 16 American Heart Association segments. Contours of RV endocardium were delineated manually in a 4-chamber long-axis slice to calculate RV longitudinal strain (RV-LS). All CMR imaging parameters were analyzed according to standard protocols by a board-certified advanced radiologist or cardiologist using dedicated software (cmr42, Circle Cardiovascular Imaging Inc).

CLINICAL AND LABORATORY ASSESSMENT. Clinical status was determined by New York Heart Association functional class, and functional exercise capacity was assessed using a 6-minute walk test in accordance with American Thoracic Society guidelines.[19] Laboratory tests included cardiac biomarkers such as serum N-terminal prohormone of brain natriuretic peptide (NT-proBNP) and troponin T, as well as hemoglobin and serum creatinine levels. The National Amyloidosis Centre (NAC) staging system,[20] which stratifies ATTR-CM patients into prognostic categories, with a higher NAC stage defining a worse outcome, was used to define disease stage.

COHORT CLASSIFICATION. Study participants were divided into 2 cohorts based on the median of the SUV retention index. ATTRwt-CM patients with an SUV retention index less than the median (<5.19 g/mL) were assigned to the *low cardiac uptake* cohort, while those with an SUV retention index equal to or greater than the median (≥5.19 g/mL) comprised the *high cardiac uptake* cohort.

STATISTICAL ANALYSIS. All statistical analyses were performed using SPSS version 29 (IBM Corp). Continuous variables are expressed as median (IQR), and categorical variables as numbers and percentages. The Mann-Whitney U test or chi-squared test was used to compare variables between groups. Univariable linear regression models were calculated to assess the associations (correlation coefficient [r], regression coefficient [β]) of the SUV retention index with clinical, laboratory, and imaging variables. Variables with significant associations were subsequently entered into a stepwise forward multiple linear regression model to adjust for potential confounding effects. The *P* values have been calculated using a 2-tailed t-test with a 2-sided significance level of alpha = 0.05 and are to be interpreted in a descriptive manner throughout.

RESULTS

STUDY PARTICIPANTS. A total of 71 treatment-naïve ATTR-CM patients underwent a comprehensive eligibility assessment, with 40 ATTRwt-CM patients undergoing DPD SPECT/CT and CMR imaging, along with clinical and laboratory assessments, were considered eligible and were assigned to the *low cardiac uptake cohort* (n = 20) or the *high cardiac uptake cohort* (n = 20); specific reasons for study exclusion or discontinuation are illustrated in Figure 1. A subset (n = 25) of eligible study participants in the present study were part of our previous publication.[8]

BASELINE CHARACTERISTICS. Detailed baseline characteristics for the entire study cohort are depicted in Table 1. ATTRwt-CM patients were elderly (78.0 years, IQR: 69.0-82.5), predominantly male (75.0%), and in an advanced stage of heart failure (NYHA functional class ≥III: 47.5%). The prevailing comorbidities included arterial hypertension (65.0%) and atrial fibrillation or flutter (42.5%). In addition, a noteworthy proportion of patients experienced neurological symptoms, including polyneuropathy (67.5%) and carpal tunnel syndrome (60.0%). Functional exercise capacity was impaired (6-minute walk distance [6MWD]: 386.5 m, IQR: 285.0 to 478.0), and cardiac biomarker analysis indicated markedly elevated levels of NT-proBNP (1,893 ng/L, IQR: 999-3,249) and troponin T (43.0 ng/L, IQR: 29.0-64.0). Prognostic stratification based on the NAC staging system categorized 62.5% of ATTRwt-CM patients in NAC stage I, 25.0% in NAC stage II, and 12.5% in NAC stage III. Nuclear imaging with DPD scintigraphy classified 27.5% of ATTRwt-CM patients as Perugini grade 2 and 72.5% as grade 3, and quantitative DPD SPECT/CT imaging demonstrated increased cardiac tracer uptake (SUV retention index: 5.2 g/mL, IQR: 3.4-6.8) (Supplemental Figure 2). CMR imaging of ATTRwt-CM patients showed pronounced interventricular septal thickness (18.0 mm, IQR: 14.9-20.4) and increased LV mass index (90.9 g/m^2, IQR: 76.1-111.9). Assessment of myocardial amyloid load by T1 mapping revealed prolonged native T1 time (1,115.0 ms, IQR: 1,079.5-1,166.3) and markedly expanded ECV (50.6%, IQR: 39.7%-57.8%). CMR analysis of cardiac function showed mildly reduced ejection fraction (EF) of the

FIGURE 1 Patient Flowchart

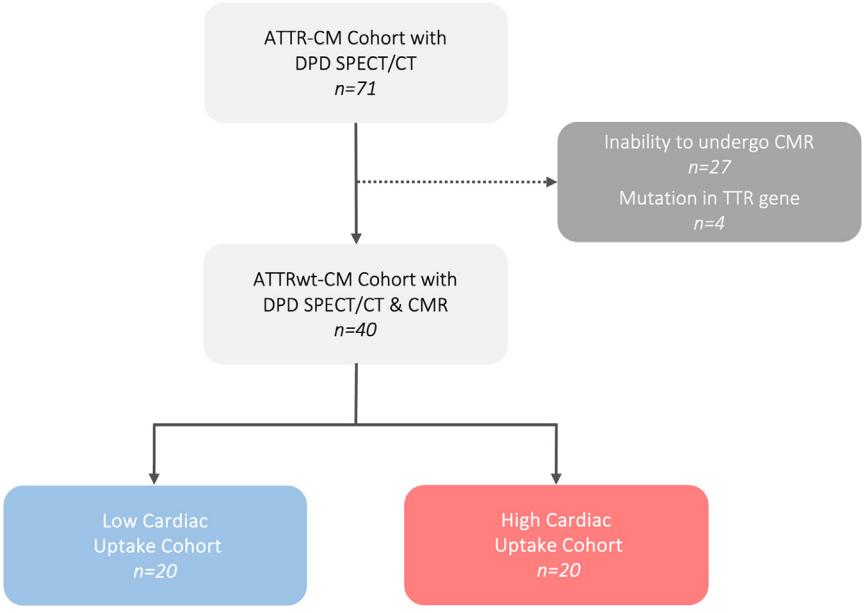

A total of 71 treatment-naïve ATTR-CM patients who underwent DPD SPECT/CT and CMR imaging were screened for the study. Reasons for study exclusion are depicted. ATTR-CM = transthyretin amyloid cardiomyopathy; ATTRwt-CM = wild-type ATTR-CM; CMR = cardiac magnetic resonance; DPD = ^{99m}Tc-3,3-diphosphono-1,2-propanodicarboxylic acid; SPECT/CT = single-photon emission computed tomography/computed tomography; TTR = transthyretin.

LV (LVEF: 47.2%, IQR: 41.6%-56.5%) and the RV (RVEF: 45.3%, IQR: 37.8%-52.5%) and impaired longitudinal cardiac function (LV-GLS: −10.9%, IQR: 13.9%-9.0%; RV-LS: −12.8%, IQR: 17.6%-10.5%). Clinical, laboratory, and imaging characteristics of the entire cohort are similar to those observed in our previous publication.[8]

COHORT COMPARISON: LOW CARDIAC UPTAKE VS HIGH CARDIAC UPTAKE. Detailed cohort comparisons are shown in **Table 1**. Comparison of CMR imaging parameters between cohorts (*low cardiac uptake vs high cardiac uptake*) revealed significant differences in myocardial amyloid load, as assessed by native T1 time (1,088.0 ms vs 1,123.0 ms, $P = 0.013$) and ECV (42.6% vs 56.3%, $P = 0.001$), as well as in RV longitudinal function (RV-LS: −14.2% vs −10.5%, $P = 0.003$). Between-cohort comparison of cardiac biomarkers yielded significant differences in serum levels of NT-proBNP (1,276 ng/L vs 3,198 ng/L, $P < 0.001$) and troponin T (40.5 ng/L vs 55.5 ng/L, $P = 0.046$), and comparison of exercise capacity revealed notable cohort differences in 6MWD (454.0 m vs 340.0 m, $P = 0.002$). In terms of prognostic stratification, significant differences in NAC stage were noted between the low cardiac uptake cohort and the high cardiac uptake cohort (NAC I: 90.0% vs 35.0%, $P < 0.001$; NAC II: 10.0% vs 40.0%, $P = 0.030$; NAC III: 0.0% vs 25.0%, $P = 0.021$).

ASSOCIATION OF DPD QUANTIFICATION WITH CARDIAC MAGNETIC RESONANCE IMAGING, CLINICAL, AND LABORATORY CHARACTERISTICS. Detailed linear regression analyses are presented in **Table 2**. Univariable linear regression analyses revealed significant associations of the SUV retention index with ECV ($r = 0.669$, $\beta = 0.139$ [95% CI: 0.088-0.189], $P < 0.001$, **Figure 2A**), native T1 time ($r = 0.432$, $\beta = 0.020$ [95% CI: 0.006-0.033], $P = 0.005$) (**Figure 2B**), and RV-LS ($r = 0.445$, $\beta = 0.204$ [95% CI: 0.069-0.339], $P = 0.004$) (**Figure 2C**), as well as NT-proBNP ($\log_{10}$) ($r = 0.458$, $\beta = 2.842$ [95% CI: 1.030-4.653], $P = 0.003$) (**Figure 3A**), troponin T ($r = 0.422$, $\beta = 0.048$ [95% CI: 0.014-0.082], $P = 0.007$) (**Figure 3B**), 6MWD ($r = 0.385$; $\beta = -0.007$ [95% CI: −0.13 to 0.001]; $P = 0.017$) (**Figure 3C**), and NAC stage ($r = 0.490$; $\beta = 1.785$ [95% CI: 0.743-2.827]; $P = 0.001$) (**Central Illustration**). After adjustment in the multiple linear regression model, significant associations of the SUV retention index with ECV ($\beta = 0.108$ [95% CI: 0.042-0.174]; $P = 0.002$) and NAC stage ($\beta = 1.745$ [95% CI: 0.536-2.954], $P = 0.006$) were observed.

TABLE 1 Baseline Characteristics and Cohort Comparison

	All Patients (N = 40)	Low Cardiac Uptake (n = 20)	High Cardiac Uptake (n = 20)	*P* Value
Clinical characteristics				
Age, y	78.0 (69.0-82.5)	79.0 (69.0-81.0)	74.0 (69.0-84.5)	0.914
Male	30 (75.0)	17 (85.0)	13 (65.0)	0.152
NYHA functional class ≥ III	19 (47.5)	7 (35.0)	12 (60.0)	0.119
6-min walk distance, m	386.5 (285.0-478.0)	454.0 (380.0-503.0)	340.0 (207.0-393.0)	**0.002**
NAC stage				
I	25 (62.5)	18 (90.0)	7 (35.0)	**<0.001**
II	10 (25.0)	2 (10.0)	8 (40.0)	**0.030**
III	5 (12.5)	0 (0.0)	5 (25.0)	**0.021**
Medical history				
Atrial fibrillation or flutter	17 (42.5)	6 (30.0)	11 (55.0)	0.115
Arterial hypertension	26 (65.0)	11 (55.0)	15 (75.0)	0.194
Coronary artery disease	13 (32.5)	8 (40.0)	5 (25.0)	0.324
Polyneuropathy	27 (67.5)	11 (55.0)	16 (80.0)	0.096
History of carpal tunnel syndrome	24 (60.0)	11 (55.0)	13 (65.0)	0.531
Medications				
Anticoagulant	19 (47.5)	8 (40.0)	11 (55.0)	0.355
Beta-blocker	13 (32.5)	7 (35.0)	6 (30.0)	0.744
ACE inhibitor	10 (25.0)	3 (15.0)	7 (35.0)	0.152
Angiotensin receptor blocker	12 (30.0)	7 (35.0)	5 (25.0)	0.503
Diuretic agent	32 (80.0)	14 (70.0)	18 (90.0)	0.121
Mineralocorticoid receptor antagonist	22 (55.0)	7 (35.0)	15 (75.0)	**0.010**
Laboratory parameters				
NT-proBNP, ng/L	1893 (999-3,249)	1,276 (683-1833)	3,198 (1952-4,701)	**<0.001**
Troponin T, ng/L	43.0 (29.0-64.0)	40.5 (28.0-56.0)	55.5 (39.0-71.0)	**0.046**
Hemoglobin, g/dL	13.8 (12.9-14.1)	14.0 (13.4-14.1)	13.7 (12.2-14.5)	0.385
Creatinine, mg/dL	1.1 (0.9-1.4)	1.0 (0.9-1.3)	1.1 (0.9-1.5)	0.394
eGFR, mL/min/1.73 m^2	64.0 (49.1-79.1)	67.9 (51.7-81.9)	59.9 (42.9-75.9)	0.213
Nuclear imaging parameters				
Perugini grade 2	11 (27.5)	8 (40.0)	3 (15.0)	0.081
Perugini grade 3	29 (72.5)	12 (60.0)	17 (85.0)	0.081
SUV retention index, g/mL	5.2 (3.4-6.8)	3.4 (2.5-3.8)	6.8 (5.9-8.5)	**<0.001**
DPD activity, MBq	725.0 (708.0-738.5)	729.0 (710.5-742.0)	721.0 (702.5-733.5)	0.543
DLP, mGy/cm	84.0 (63.3-99.0)	83.5 (64.0-92.0)	84.0 (61.0-112.0)	0.627
CMR imaging parameters				
Extracellular volume, %	50.6 (39.7-57.8)	42.6 (33.8-52.2)	56.3 (46.0-62.2)	**0.001**
Native T1 time, ms	1,115.0 (1,079.5-1,166.3)	1,088.0 (1,049.5-1,133.0)	1,123.0 (1,100.0-1,177.5)	**0.013**
Interventricular septum, mm	18.0 (14.9-20.4)	17.1 (14.2-20.0)	18.4 (15.6-20.4)	0.379
LV mass index, g/m^2	90.9 (76.1-111.9)	93.4 (76.1-108.3)	90.2 (76.8-114.6)	0.935
LV ejection fraction, %	47.2 (41.6-56.5)	47.1 (41.5-59.0)	47.6 (42.1-56.5)	0.957
LV cardiac index, L/min/m^2	2.9 (2.4-3.4)	3.1 (2.5-3.3)	2.5 (2.3-3.4)	0.250
LV global longitudinal strain, -%	10.9 (13.9-9.0)	12.4 (14.0-10.4)	9.8 (13.3-8.8)	0.117
RV ejection fraction, %	45.3 (37.8-52.5)	46.1 (39.0-54.7)	42.6 (36.8-51.1)	0.239
RV cardiac index, L/min/m^2	2.5 (2.1-3.1)	2.6 (2.2-3.6)	2.5 (2.1-3.0)	0.473
RV longitudinal strain, -%	12.8 (17.6-10.5)	14.2 (18.2-12.5)	10.5 (13.4-7.5)	**0.003**

Values are median (IQR) or n (%). **Bold** indicates $P \leq 0.05$.

ACE = angiotensin-converting enzyme; CMR = cardiac magnetic resonance; DPD = ^{99m}Tc-3,3-diphosphono-1,2-propanodicarboxylic acid; DLP = dose length product; eGFR = estimated glomerular filtration rate; LV = left ventricle; NAC = National Amyloidosis Centre; NT-proBNP = N-terminal prohormone of brain natriuretic peptide; NYHA = New York Heart Association; RV = right ventricle; SUV = standardized uptake value.

DISCUSSION

Quantitative DPD SPECT/CT imaging may aid in quantifying and monitoring cardiac disease burden and in assessing changes in response to disease-specific therapies in ATTRwt-CM.[6-8,21] However, the relationship between quantitative cardiac tracer uptake and amyloid load in the myocardium is barely investigated.[13,14] This is the first study to systematically investigate the associations between DPD

TABLE 2 Linear Regression Analyses for the SUV Retention Index and Clinical, Laboratory, and Imaging Parameters (N = 40)

	Univariable Model			Multivariable Model	
	r	β (95% CI)	*P* Value	β (95% CI)	*P* Value
NYHA functional class	0.204	0.678 (−0.391 to 1.747)	0.207		
6-minute walk distance	0.385	−0.007 (−0.13 to 0.001)	**0.017**	−0.002 (−0.007 to 0.003)	0.433
NAC stage	0.490	1.785 (0.743-2.827)	**0.001**	1.745 (0.536-2.954)	**0.006**
Log_{10} NT-proBNP	0.458	2.842 (1.030-4.653)	**0.003**	−0.381 (−2.353 to 1.591)	0.696
Troponin T	0.422	0.048 (0.014-0.082)	**0.007**	−0.009 (−0.045 to 0.027)	0.615
Extracellular volume	0.669	0.139 (0.088-0.189)	**<0.001**	0.108 (0.042-0.174)	**0.002**
Native T1 time	0.432	0.020 (0.006-0.033)	**0.005**	−0.002 (−0.014 to 0.010)	0.737
Interventricular septum	0.250	0.143 (−0.039 to 0.324)	0.120		
LV mass index	0.295	0.028 (−0.002 to 0.058)	0.064		
LV ejection fraction	0.087	−0.019 (−0.091 to 0.053)	0.595		
LV cardiac index	0.163	−0.496 (−1.483 to 0.492)	0.316		
LV global longitudinal strain	0.161	0.110 (−0.111 to 0.331)	0.322		
RV ejection fraction	0.183	−0.046 (−0.127 to 0.035)	0.257		
RV cardiac index	0.061	0.183 (−0.793 to 1.159)	0.707		
RV longitudinal strain	0.445	0.204 (0.069-0.339)	**0.004**	0.093 (−0.019 to 0.205)	0.099

r indicates correlation coefficient. β indicates regression coefficient. **Bold** indicates $P \leq 0.05$.
Abbreviations as in Table 1.

quantification on SPECT/CT and myocardial amyloid burden assessed by CMR imaging, along with cardiac function, cardiac biomarkers, and clinical status in patients with ATTRwt-CM. We demonstrated that: (I) Quantitative cardiac DPD uptake, as measured by SUV retention index, correlated with myocardial amyloid load as assessed by CMR-derived ECV, longitudinal cardiac function, cardiac biomarkers, exercise capacity, and disease stage. (II) Comparison of low and high cardiac uptake cohorts, classified by median SUV retention index, indicating advanced disease severity in ATTRwt-CM patients with enhanced quantitative cardiac DPD uptake. Therefore, DPD quantification may provide a valuable tool for quantifying and monitoring cardiac disease burden in patients with ATTRwt-CM.

Nuclear imaging with quantitative SPECT/CT using amyloid-avid tracers has emerged as an advanced noninvasive diagnostic tool in ATTR-CM, utilizing 3-dimensional visualization of tracer uptake in the body with determination of SUV, and may therefore be valuable to quantify and monitor myocardial amyloid burden.[6-8] In the present study, 40 ATTRwt-CM patients underwent quantitative DPD SPECT/CT and CMR imaging, and we observed significant associations of the SUV retention index with ECV ($P < 0.001$) and native T1 time ($P = 0.005$). T1 mapping-derived ECV is generally a marker of extracellular matrix alterations and has already been validated for its association with cardiac amyloid burden,[22] with a strong correlation to amyloid in the extracellular matrix of endomyocardial tissue samples from ATTR-CM patients.[11,12] Furthermore, ECV is an independent prognostic factor for outcome in this patient population.[9,23] Evidence for an association between cardiac amyloid burden and myocardial DPD uptake on planar bone scintigraphy was provided by Hutt et al, who reported a significant difference in CMR-derived ECV between ATTR-CM patients with distinct Perugini grades.[24] Moreover, the findings of the present study are also consistent with those reported by Dorbala et al[13] and Avalon et al,[14] in which a subset of 11 and 9 patients with ATTRwt-CM undergoing ^{99m}Tc-pyrophosphate (PYP) SPECT/CT and CMR imaging demonstrated a strong positive correlation of SUV-max with ECV, suggesting that DPD, along with PYP, serves as a valuable amyloid-avid tracer to quantify myocardial amyloid burden in ATTRwt-CM and may be predictive of outcome.

In addition to LV infiltration, amyloid fibril deposition is also expected in the RV of ATTRwt-CM patients, leading to increased stiffness and progressive loss of function.[25] In the present study, we identified notable associations between the SUV retention index and RV-LS ($P = 0.004$), which indicates that higher quantitative cardiac DPD uptake is associated with more severe impairment of longitudinal cardiac function.

In previous studies, elevated levels of cardiac biomarkers, including troponin T and NT-proBNP, have been associated with adverse outcomes in patients with ATTRwt-CM, whether assessed individually or in combination.[26] Data from a PYP planar imaging study correlating semiquantitative metrics like the heart-to-contralateral lung uptake (H/CL) ratio with cardiac biomarkers demonstrated a robust association with

FIGURE 2 Correlation: DPD Quantification and CMR Imaging Characteristics

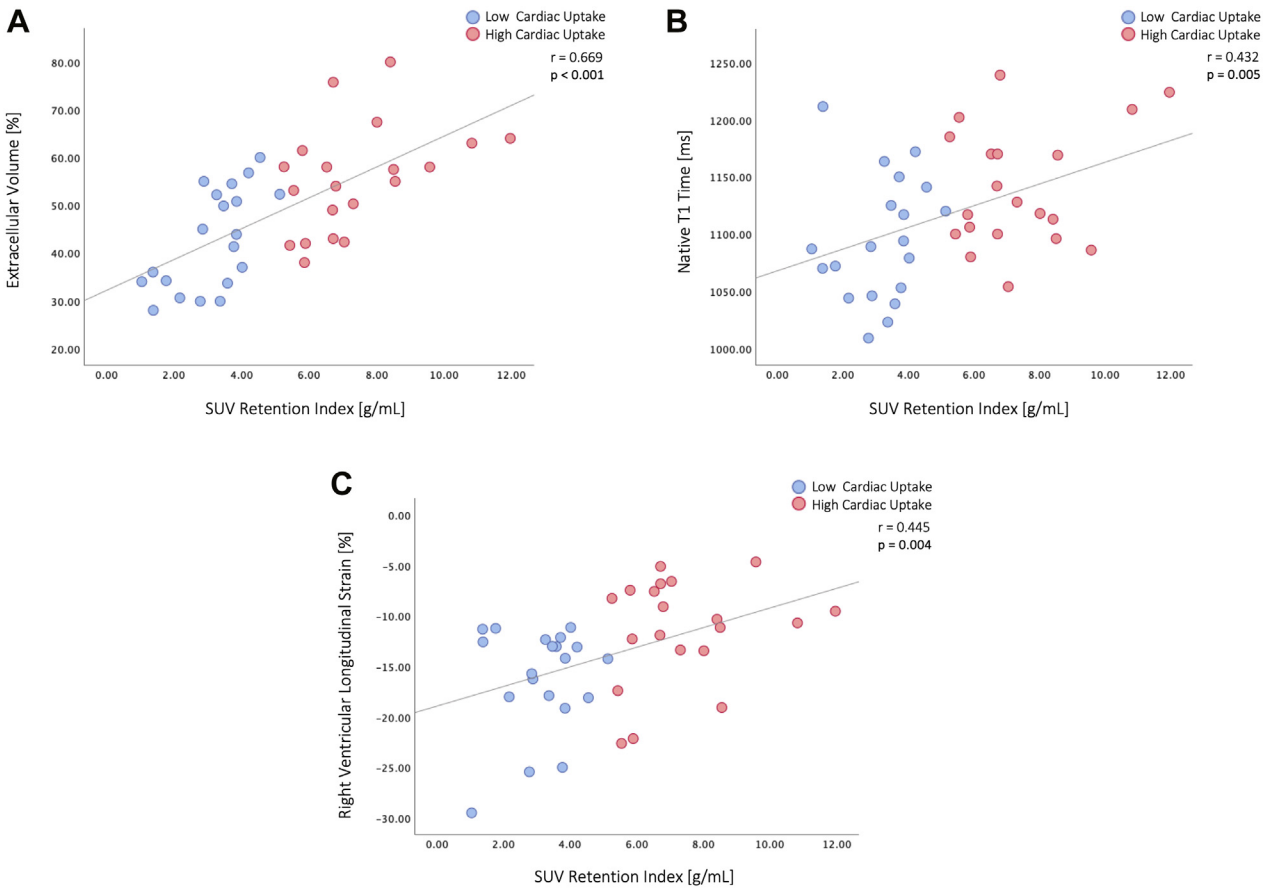

(A) Correlation between SUV retention index and extracellular volume. (B) Correlation between SUV retention index and native T1 time. (C) Correlation between SUV retention index and right ventricular longitudinal strain. CMR = cardiac magnetic resonance; DPD = ^{99m}Tc-3,3-diphosphono-1,2-propanodicarboxylic acid; SUV = standardized uptake value.

troponin T, however not with NT-proBNP.[27] In contrast, in our study, we observed significant correlations of the SUV retention index with troponin T ($P = 0.007$) and NT-proBNP ($P = 0.003$), emphasizing the sensitivity of quantitative over semiquantitative imaging approaches.

Individuals with CA not only suffer from elevated cardiac biomarkers but also from diminished exercise capacity, particularly in advanced stages of disease, as demonstrated by imaging studies investigating the relationship between myocardial amyloid burden and exercise capacity, where increasing ECV correlated with poorer 6MWD performance.[10,28] This was also seen in our study, in which the SUV retention index negatively correlated with 6MWD ($P = 0.017$), indicating that higher quantitative cardiac DPD uptake is associated with worse exercise capacity in ATTRwt-CM patients.

In general, CA face a poor prognosis, which can be evaluated using a prognostic staging system that stratifies ATTR-CM patients into prognostic categories, with a higher NAC stage defining a worse outcome.[20] In the present study, we observed a positive association between quantitative cardiac DPD uptake and NAC stage ($P = 0.001$), suggesting that the SUV retention index may have prognostic value in ATTRwt-CM.

Comparison of the low and high cardiac uptake cohorts implies advanced disease severity in ATTRwt-CM patients with enhanced quantitative cardiac DPD uptake, which is particularly evident in terms of myocardial amyloid load (ECV: $P = 0.001$,

FIGURE 3 **Correlation: DPD Quantification and Clinical and Laboratory Characteristics**

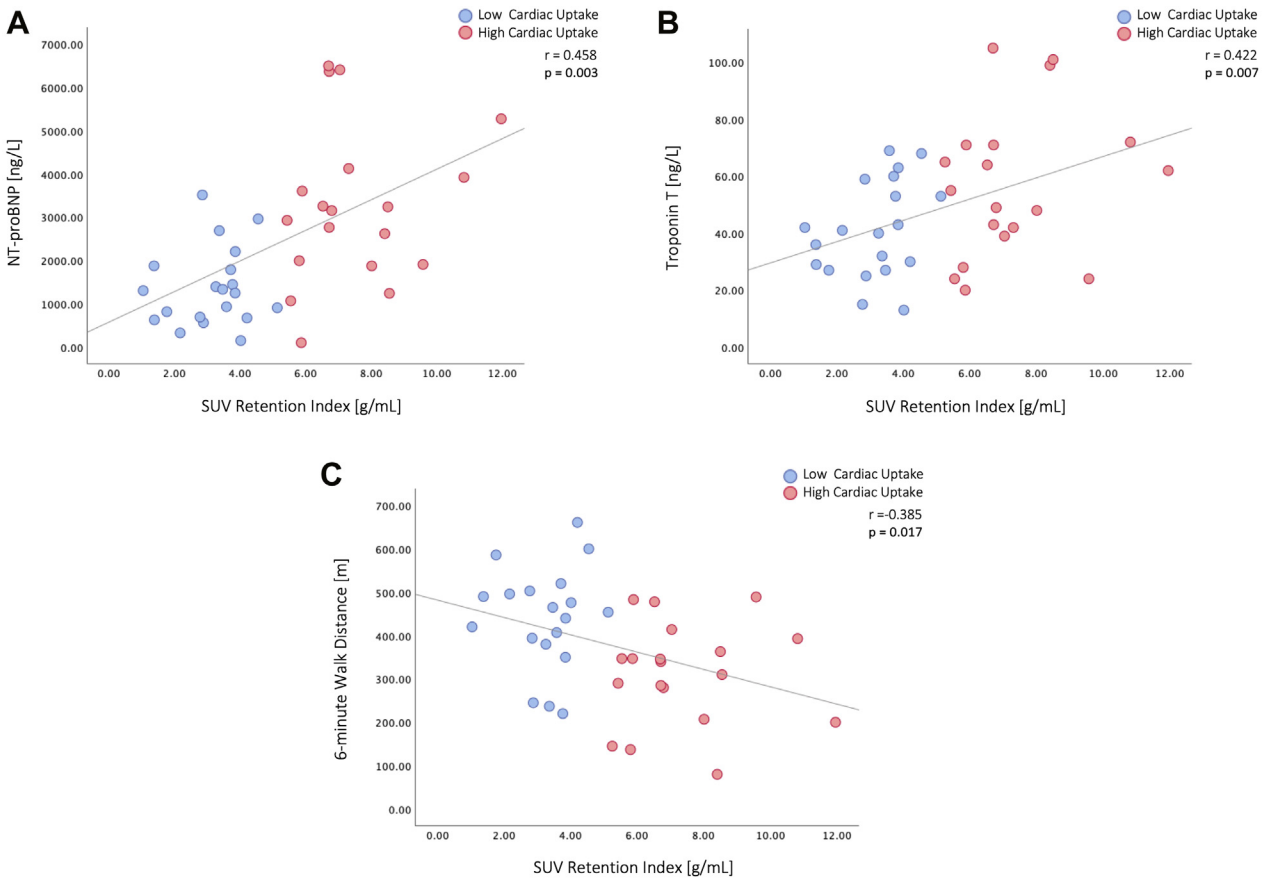

(A) Correlation between SUV retention index and NT-proBNP. (B) Correlation between SUV retention index and troponin T. (C) Correlation between SUV retention index and 6-minute walk distance. DPD = ^{99m}Tc-3,3-diphosphono-1,2-propanodicarboxylic acid; NT-proBNP = N-terminal prohormone of brain natriuretic peptide; SUV = standardized uptake value.

native T1 time: $P = 0.013$), longitudinal cardiac function (RV-LS: $P = 0.003$), cardiac biomarkers (NT-proBNP: $P < 0.001$, troponin T: $P = 0.046$), exercise capacity (6MWD: $P = 0.002$), and disease stage (NAC stage, I: $P < 0.001$, II: $P = 0.030$, III: $P = 0.021$). These findings suggest that DPD quantification may serve as a valuable tool for quantifying and monitoring cardiac disease burden in ATTRwt-CM.

Further long-term studies are warranted to investigate the relationship between quantitative cardiac DPD uptake and outcome in patients with ATTRwt-CM and will demonstrate whether highly disease-specific SPECT/CT with amyloid-avid tracers is more sensitive than established imaging modalities for monitoring disease progression and outcome.

This would also allow for a better understanding of effects of novel treatment strategies for ATTRwt-CM.

STUDY LIMITATIONS. The current study is subject to certain limitations that merit discussion. Firstly, due to the single-center design of our study, a center-specific bias cannot be excluded. However, restricting data collection to one center offers notable benefits in terms of maintaining consistency in diagnostic work-up, clinical routine, and imaging procedures. Secondly, the sample size is limited, mainly due to the rarity of ATTRwt-CM, and given the lack of control for family-wise error rates, the results of the present study should be interpreted

CENTRAL ILLUSTRATION **Correlation of DPD Quantification With Myocardial Amyloid Burden, Longitudinal Cardiac Function, Cardiac Biomarkers, Exercise Capacity, and Disease Stage in ATTRwt-CM**

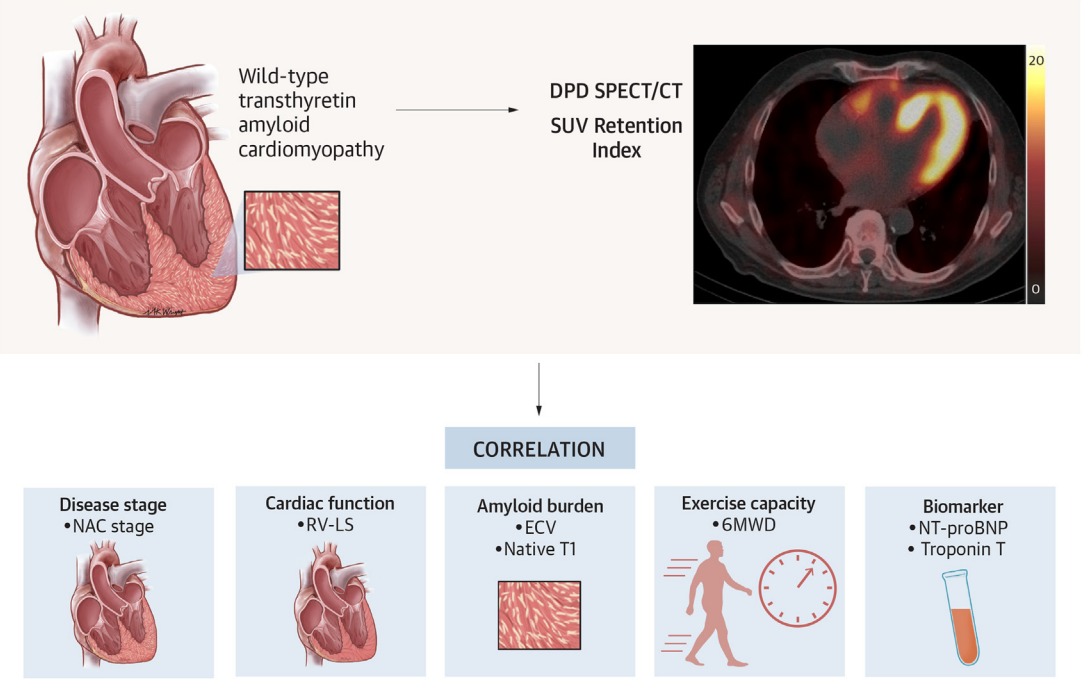

Rettl R, et al. JACC Adv. 2024;3(10):101261.

6MWD = 6-minute walk distance; ATTRwt-CM = wild-type transthyretin amyloid cardiomyopathy; DPD = ^{99m}Tc-3,3-diphosphono-1,2-propanodicarboxylic acid; ECV = extracellular volume; NAC = National Amyloidosis Centre; NT-proBNP = N-terminal prohormone of brain natriuretic peptide; RV-LS = right ventricular longitudinal strain; SPECT/CT = single-photon emission computed tomography/computed tomography; SUV = standardized uptake value.

with caution. However, this study has made a significant contribution to the existing literature. Thirdly, the study cohort was not reflective of the overall ATTRwt-CM patient population, as patients with contraindications to CMR imaging and therefore potentially at a more advanced disease stage were excluded. However, this is the first study to systematically compare quantitative DPD SPECT/CT acquisitions with imaging outcomes in patients with ATTRwt-CM. Fourthly, although the SUV retention index correlates with ECV and thus with myocardial amyloid load, this has not yet been histologically validated. However, the main findings of the study are consistent with previously published data. Finally, the observation period was too short to assess the relationship between quantitative cardiac DPD uptake and outcome.

CONCLUSIONS

In patients with ATTRwt-CM, quantitative cardiac DPD uptake correlates with myocardial amyloid load, longitudinal cardiac function, cardiac biomarkers, exercise capacity, and disease stage, and enhanced cardiac DPD uptake is indicative of advanced disease severity. Therefore, DPD quantification may provide a valuable tool for quantifying and monitoring cardiac disease burden in affected individuals. Further studies are warranted to investigate the prognostic implications of quantitative cardiac DPD uptake in ATTRwt-CM.

FUNDING SUPPORT AND AUTHOR DISCLOSURES

Dr Rettl has received speaker fees and congress support from Akcea Therapeutics, Alnylam Pharmaceuticals, and Pfizer Inc, as well as

research grants from Pfizer Inc. Dr Duca has received speaker fees and congress support from AOP Orphan Pharmaceuticals GmbH, Alnylam Pharmaceuticals, Bayer AG, Novartis AG, Pfizer Inc and, as well as research grants from the Austrian Society of Cardiology and Pfizer Inc. Dr Beitzke has received speaker fees from GE Healthcare and Siemens. Dr Nitsche receives speaker fees and research grants from Pfizer Inc. Dr Badr Eslam has received speaker fees from Merck Sharp & Dohme Ges.m.b.H., AOP Orphan Pharmaceuticals GmbH, and OrphaCare GmbH, as well as research grants from OrphaCare GmbH and Astra Zeneca GmbH. All other authors have reported that they have no relationships relevant to the contents of this paper to disclose.

ADDRESS FOR CORRESPONDENCE: Dr Andreas Anselm Kammerlander, Division of Cardiology, Department of Internal Medicine II, Medical University of Vienna, Waehringer Guertel 18-20, Vienna 1090, Austria. E-mail: andreas.kammerlander@meduniwien.ac.at.

PERSPECTIVES

COMPETENCY IN MEDICAL KNOWLEDGE: Disease-specific SPECT/CT imaging with DPD quantification as part of a routine assessment will broaden the diagnostic approach of established imaging modalities and aid in quantifying and monitoring cardiac disease burden in patients with ATTRwt-CM.

TRANSLATIONAL OUTLOOK: Extended, long-term studies may help to assess the relationship between quantitative cardiac DPD uptake and outcome in patients with ATTRwt-CM and will demonstrate whether highly disease-specific SPECT/CT with amyloid-avid tracers is more sensitive than established imaging modalities for monitoring disease progression and outcome. This would also provide a broader understanding of the impact of novel treatment approaches in ATTRwt-CM.

REFERENCES

1. Ruberg F, Berk J. Transthyretin (TTR) cardiac amyloidosis. *Circulation*. 2012;126(10):1286-1300.

2. Gertz MA, Benson MD, Dyck PJ, et al. Diagnosis, prognosis, and therapy of transthyretin amyloidosis. *J Am Coll Cardiol*. 2015;66(21):2451-2466.

3. Perugini E, Guidalotti PL, Salvi F, et al. Noninvasive etiologic diagnosis of cardiac amyloidosis using 99mTc-3,3-diphosphono-1,2-propanodicarboxylic acid scintigraphy. *J Am Coll Cardiol*. 2005;46(6):1076-1084.

4. Gillmore JD, Maurer MS, Falk RH, et al. Nonbiopsy diagnosis of cardiac transthyretin amyloidosis. *Circulation*. 2016;133(24):2404-2412.

5. Dorbala S, Ando Y, Bokhari S, et al. ASNC/AHA/ASE/EANM/HFSA/ISA/SCMR/SNMMI expert consensus recommendations for multimodality imaging in cardiac amyloidosis: Part 1 of 2—evidence base and standardized methods of imaging. *Circ Cardiovasc Imaging*. 2021;14(7):e000029.

6. Scully PR, Morris E, Patel KP, et al. DPD quantification in cardiac amyloidosis. *JACC Cardiovasc Imaging*. 2020;13(6):1353-1363.

7. Wollenweber T, Rettl R, Kretschmer-Chott E, et al. In vivo quantification of myocardial amyloid deposits in patients with suspected transthyretin-related amyloidosis (ATTR). *J Clin Med*. 2020;9(11):1-13.

8. Rettl R, Wollenweber T, Duca F, et al. Monitoring tafamidis treatment with quantitative SPECT/CT in transthyretin amyloid cardiomyopathy. *Eur Heart J Cardiovasc Imaging*. 2023;24(8):1019-1030.

9. Martinez-Naharro A, Treibel TA, Abdel-Gadir A, et al. Magnetic resonance in transthyretin cardiac amyloidosis. *J Am Coll Cardiol*. 2017;70(4):466-477.

10. Martinez-Naharro A, Kotecha T, Norrington K, et al. Native T1 and extracellular volume in transthyretin amyloidosis. *JACC Cardiovasc Imaging*. 2019;12(5):810-819.

11. Kammerlander AA, Marzluf BA, Zotter-Tufaro C, et al. T1 mapping by CMR imaging from histological validation to clinical implication. *JACC Cardiovasc Imaging*. 2016;9(1):14-23.

12. Duca F, Kammerlander AA, Panzenböck A, et al. Cardiac magnetic resonance T1 mapping in cardiac amyloidosis. *JACC Cardiovasc Imaging*. 2018;11(12):1924-1926.

13. Dorbala S, Park MA, Cuddy S, et al. Absolute quantitation of cardiac ^{99m}Tc-pyrophosphate using cadmium-zinc-telluride-based SPECT/CT. *J Nucl Med*. 2021;62(5):716-722.

14. Avalon JC, Fuqua J, Deskins S, et al. Quantitative single photon emission computed tomography derived standardized uptake values on 99mTc-PYP scan in patients with suspected ATTR cardiac amyloidosis. *J Nucl Cardiol*. 2023;30(1):127-139.

15. Vija A. Introduction to xSPECT technology: evolving multi-modal SPECT to become context-based and quantitative. *White Pap*. 2013:1-28.

16. Ramsay SC, Lindsay K, Fong W, Patford S, Younger J, Atherton J. Tc-HDP quantitative SPECT/CT in transthyretin cardiac amyloid and the development of a reference interval for myocardial uptake in the non-affected population. *Eur J Hybrid Imaging*. 2018;2(1):17.

17. Kramer CM, Barkhausen J, Bucciarelli-Ducci C, Flamm SD, Kim RJ, Nagel E. Standardized cardiovascular magnetic resonance imaging (CMR) protocols: 2020 update. *J Cardiovasc Magn Reson*. 2020;22(1):17.

18. Kellman P, Wilson JR, Xue H, Ugander M, Arai AE. Extracellular volume fraction mapping in the myocardium, part 1: evaluation of an automated method. *J Cardiovasc Magn Reson*. 2012;14(1):63.

19. ATS Committee on Proficiency Standards for Clinical Pulmonary Function Laboratories. ATS statement: guidelines for the six-minute walk test. *Am J Respir Crit Care Med*. 2002;166(1):1-7.

20. Gillmore JD, Damy T, Fontana M, et al. A new staging system for cardiac transthyretin amyloidosis. *Eur Heart J*. 2018;39(30):2799-2806.

21. Rettl R, Calabretta R, Duca F, et al. Reduction in ^{99m}Tc-DPD myocardial uptake with therapy of ATTR cardiomyopathy. *Amyloid*. 2024;31(1):42-51.

22. Rettl R, Mann C, Duca F, et al. Tafamidis treatment delays structural and functional changes of the left ventricle in patients with transthyretin amyloid cardiomyopathy. *Eur Heart J Cardiovasc Imaging*. 2022;23(6):767-780.

23. Duca F, Rettl R, Kronberger C, et al. Myocardial structural and functional changes in cardiac amyloidosis: insights from a prospective observational patient registry. *Eur Heart J Cardiovasc Imaging*. 2023;25(1):95-104.

24. Hutt DF, Fontana M, Burniston M, et al. Prognostic utility of the Perugini grading of 99mTc-DPD scintigraphy in transthyretin (ATTR)

amyloidosis and its relationship with skeletal muscle and soft tissue amyloid. *Eur Heart J Cardiovasc Imaging*. 2017;18(12):1344–1350.

25. Arvidsson S, Henein MY, Wikström G, Suhr OB, Lindqvist P. Right ventricular involvement in transthyretin amyloidosis. *Amyloid*. 2018;25(3):160–166.

26. Grogan M, Scott CG, Kyle RA, et al. Natural history of wild-type transthyretin cardiac amyloidosis and risk stratification using a novel staging system. *J Am Coll Cardiol*. 2016;68(10):1014–1020.

27. Morioka M, Takashio S, Nakashima N, et al. Correlation between cardiac images, biomarkers, and amyloid load in wild-type transthyretin amyloid cardiomyopathy. *J Am Heart Assoc*. 2022;11(12):e024717.

28. Banypersad SM, Sado DM, Flett AS, et al. Quantification of myocardial extracellular volume fraction in systemic AL amyloidosis. *Circ Cardiovasc Imaging*. 2013;6(1):34–39.

KEY WORDS ATTR amyloidosis, ATTRwt-CM, CMR, ECV, SPECT/CT

APPENDIX For supplemental figures, please see the online version of this paper.